AD-A040 336 INTERNATIONAL NICKEL CO INC NEW YORK F/G 9/1
NICKEL COMPOSITE MAGNETOSTRICTIVE MATERIAL RESEARCH FOR ULTRASO--ETC(U)
JAN 77 D T PETERS, E L HUSTON N00039-76-C-0017

UNCLASSIFIED NL

| OF |
AD
A040336

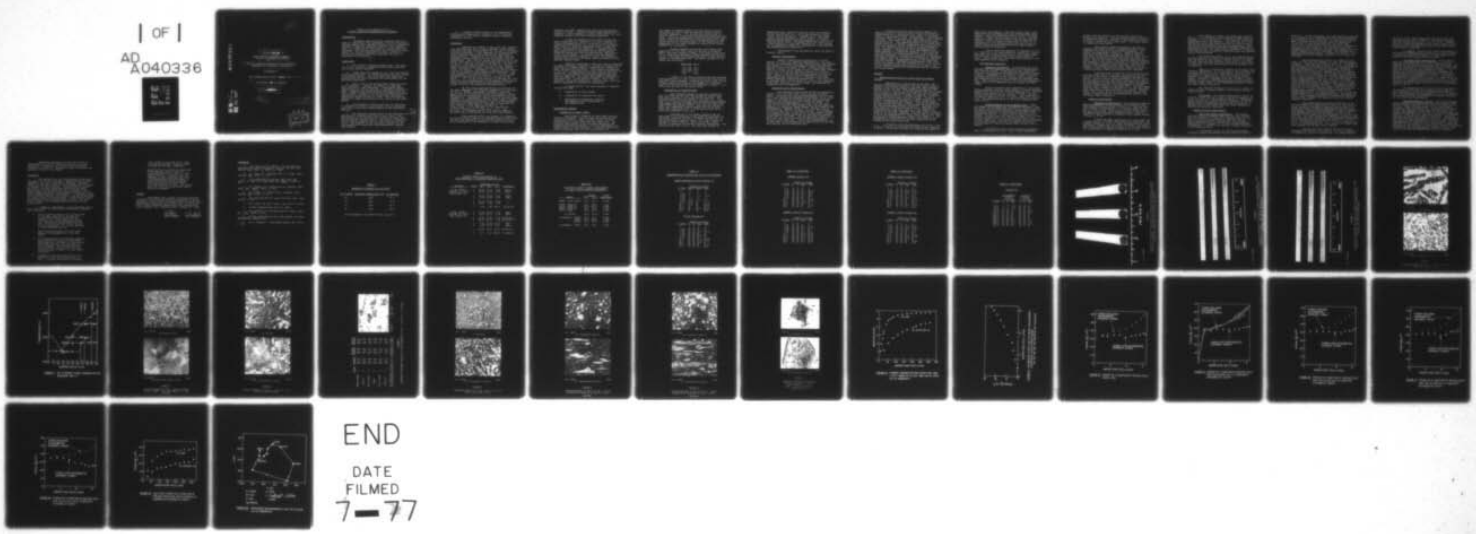

END
DATE
FILMED
7-77

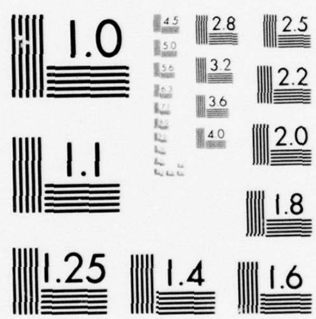
1.0
1.1
1.25
1.4
1.6
1.8
2.0
2.2
2.5
2.8
3.2
3.6
4.0
4.5
5.0
5.6

12
B.S.

9 Final Rep[redacted]t, [redacted]

Naval Electronic Systems Command
Contract No. 15 N00039-76-C-0017 New

6 "Nickel Composite Magnetostrictive Material
Research for Ultrasonic Transducer"

Performed by

The International Nickel Company, Inc. New York, N.Y.

10 D.T. Peters [redacted] E.L. Huston

11 Jan[redacted]977

12 42p.

187 050

A STUDY OF THE FEASIBILITY OF A Ni/$SmFe_2$ COMPOSITE MAGNETOSTRICTIVE MATERIAL

INTRODUCTION

This report describes basic research under Contract No. N00039-76-C-0017 sponsored by the Naval Electronic Systems Command. The immediate objective was to manufacture and test a composite transducer material of the compound $SmFe_2$ in a nickel matrix fabricated by a powder metallurgy technique. The long term objective was the effective utilization of a 'giant' magnetostrictive $REFe_2$ material in a ductile and corrosion resistant composite for use as a transducer core material.

CONCLUSIONS

1. The Ni/Sm-Fe composites showed only a very small (12 to 20%) increase in magnetostrictive strain over the pure nickel control specimen.

2. Powder extrusion appears to be a very satisfactory fabrication procedure. The Sm-Fe particles were well bonded to the nickel matrix. The nickel matrix was completely densified and the Sm-Fe particles are quite plastic at the extrusion temperature.

3. Very little of the desired $SmFe_2$ phase was found in the composite. Instead, the higher iron compounds $SmFe_3$ and Sm_2Fe_{17} were identified. These phases reduce magnetostriction and are difficult to magnetize compared to $SmFe_2$. Samarium loss during melting and annealing is the basic problem. Because of the melting procedure originally used to make the Sm-Fe alloy, the particles contained a substantial volume fraction of voids. The voids would be expected to reduce the coupling of the strain to the nickel matrix.

4. The dispersion of Sm-Fe particles (10 and 20 wt. %) hardened the nickel to some extent, but the composites were found to have good tensile ductility and were easily machined.

5. The saturation magnetization of the composites was only slightly different from that of pure nickel. The permeability of the composites was found to be lower than that of the pure nickel control. The resonant frequency of the Ni/20%Sm-Fe composite was 15% lower than that of pure nickel. The geometry of the test bars available did not lend themselves to meaningful electromechanical coupling measurements.

6. A number of modifications to the experimental procedures are suggested to eliminate the difficulties experienced in this initial attempt at such a composite transducer material.

BACKGROUND

Compounds of a number of rare earth (RE) elements with iron have been shown to have extremely large magnetostrictions and thus are candidates for the core of a magnetostrictive transducer. These compounds are characterized by large magnetocrystalline anisotropies and high magnetic saturation(1,2). Compounds of the formula $REFe_2$ have the strongest exchange interactions and the highest ordering temperatures. $TbFe_2$ has the largest magnetostriction of the family (2630 ppm), but very large values were also measured for Tb_2Fe_{17} (194 ppm) and $TbFe_3$ (1040 ppm)(3). The immensity of these magnetostrictions is seen when compared to random polycrystalline nickel (-55 ppm) or cube textured nickel (-85 ppm)(4). Replacement of the Tb with Sm leads to a series of compounds with negative magnetostriction. The $SmFe_2$ compound has a magnetostriction of -2340 ppm. These magnetostriction values are given as λ $-\lambda$ at 25 kOe for the RE-Fe compounds and a few tens of oersteds for the nickel. λ $-\lambda$ is the strain parallel to the magnetic field minus the strain perpendicular to the magnetic field and in random polycrystalline materials and sufficiently large fields is 3/2 λ_s, the saturation magnetostriction.

The very high magnetocrystalline anisotropies of the $REFe_2$ compounds ($>10^7$ ergs-cm^3 compared to 5×10^4 ergs-cm^3 for Ni) present considerable problems to practical application of the materials as very large magnetic fields employing bulky windings and large power supplies would be necessary(5). "Compensated" alloys involving two rare earth elements, one having positive and the other negative magnetocrystalline anisotropy constants K_1 and K_2 in the compound with iron, have been shown to give lower anisotropies and thus respond to lower magnetic fields(6,7). In $Tb_xDy_{(1-x)}Fe_2$, $|K|$ is less than 5×10^5 ergs-cm^2 and λ $-\lambda$ is about 1600 ppm at H = 25 kOe and x = 0.27. The $Sm_{0.88}Dy_{0.12}Fe_2$ compound having large negative magnetostriction and low anisotropy has also been identified(8).

Other problems facing the designer in attempting to utilize a RE-Fe compound in a magnetostrictive device are the very poor mechanical properties and extremely low corrosion resistance of the materials in fresh or salt water.

Generally the $REFe_2$ compounds are glass brittle and quite reactive in water. Designs providing large compressive stresses to avoid fracture in tension would have to be used. Complete isolation from water would be essential.

It was the objective of this work to test the basic feasibility of a composite of a RE-Fe compound in a ductile ferromagnetic matrix. Because of its corrosion resistance and ductility, nickel was chosen as the matrix. $SmFe_2$, having a negative magnetostriction, as does the nickel, was chosen as the compound. A composite having $SmFe_2$ particles in a continuous matrix was envisioned. Mechanical properties would be substantially improved by virtue of this design. In addition, the ferromagnetic matrix phase would be expected to amplify the externally applied field acting on the $SmFe_2$ particles because of the internal Lorentz field.

Composite structures of this type can be fabricated by powder metallurgy techniques. The key to success lies in achieving an intimate bonding (interdiffusion) between the $REFe_2$ particles and the matrix. This assures transmission of the "giant" magnetostrictive strain from the particles to the matrix. Net magnetostriction then depends upon the amount (volume fraction) of the $REFe_2$ phase incorporated into the composite. The powder metallurgical variables of importance are: volume fraction of $REFe_2$, size of the particles, sintering temperature, sintering time, and final density expressed as a percent of theoretical.

In broad outline, the tasks required to complete this project were:

A. Preparation of $SmFe_2$ powder.

B. Preparation of composite bar stock.

C. Measurement of mechanical, magnetic and magnetostrictive properties of the composite bar.

EXPERIMENTAL METHODS

Preparation of $SmFe_2$ Powder

Four pounds of samarium in chunk form were purchased from Molycorp. The iron used was Glidden A-100-B containing 0.003%C, 0.012%S, 0.001%P, 0.X%Ni, 0.021%O, 0.0026%N and all other impurities less than 0.01%. The materials were weighed to the intended composition and tungsten electrode arc melted in an argon atmosphere on a copper hearth as 50-gram buttons. To minimize loss of the volatile samarium, the iron was first melted, and the chunks of samarium pushed into the liquid iron pool. The button was then turned and remelted several times to increase homogeneity. The buttons were annealed for 24 hours at 850°C in a Vycor tube evacuated and backfilled with argon. Obtaining homogeneous buttons that were mostly $SmFe_2$ proved to be very difficult and is discussed below in some detail because of the significance of the composition and homogeneity of the Sm-Fe compound in achieving the overall objective of the project.

Buttons prepared in this way, and thought from examination of the first couple of buttons to be mostly $SmFe_2$, were then crushed to powder in an argon-filled glove box to prevent the pyrophoric excess samarium from burning in air. The powder was screened through a 60 mesh sieve to remove the coarsest particles. The screen analysis of the powder was as follows:

Mesh Size	Wt. %
- 60 +150	49.1
-150 +200	15.4
-200 +325	15.6
-325	19.9

A number of the first buttons melted were examined metallographically in the as-cast condition and after the 24 hour/850°C heat treatment. Grinding was done on dry silicon carbide papers and polishing with diamond in a kerosene carrier to avoid corrosion of the specimens in water. A 2% nital etch was used on the Sm-Fe alloys.

Preparation of Composite Rods

Five 1000-gram charges of the $SmFe_2$ powder and type 123 nickel powder were wire blended in sealed glass jars after weighing in the argon-filled glove box. The blended powders were then sealed in 1.5-inch O.D. x 1.25-inch I.D. x 4-inch long copper cans fabricated from standard size copper pipe and a bottom disc cut from 1/8-inch thick copper plate and heliarc welded. The cans were sealed in argon until immediately before welding the top in place. Three cans containing 10 wt. % Sm-Fe and two with 20 wt. % Sm-Fe were prepared in this way.

Consolidation of the powder composite was accomplished by hot extrusion of the powder mix protected by the copper container through a 7/16-inch diameter die. A 750-ton extrusion press was used. The 10 wt. % blend was extruded at 1200°F (649°C), 1400°F (760°C) and 1600°F (871°C) to establish the optimum extrusion temperature. The extrusion ratio was 11.75:1. The cans were brought to temperature over a period of one hour prior to extrusion. One can containing 20 wt. % Sm-Fe was extruded at 1400°F (760°C) with no difficulty. A second can at this higher loading stalled the press at 1200°F (649°C). This composition would probably extrude successfully at 1200°F at a lower extrusion ratio. The copper sheath was turned off in a lathe leaving 1/4-inch (6mm) diameter rod. This rod was cut to appropriate lengths for measurements of the magnetic and magnetostrictive properties.

Photographs of the extruded bar stock are shown in Figures 1 and 2.

Magnetic Measurements

Magnetic moments were determined on 0.1-gram samples in a null coil pendulum magnetometer(9), the specimen and its surrounding coil were located between the tapered pole faces of a 7-inch electromagnet capable of producing magnetic fields up to about 12 kOe. B-H measurements were made on a 6-inch (15 cm) length of the 1/4-inch (6mm) diameter rod of the Ni-20% Sm-Fe composite located in a 200-turn search coil in a 20-inch long solenoid having 51 turns per inch. Fields to 300 Oe could be generated in this coil. Measurements were made by the d.c. ballistic flux meter method described in ASTM Test Method A-341. A B-H curve for an annealed Nickel 270 rod which is a high purity commercial nickel made from type 123 nickel powder, was obtained for comparison with the composite.

Magnetostrictive Measurements

The magnetostrictive length change was measured on lengths of the 1/4-inch (6mm) bar by the use of strain gauges. The gauge used was Micro-Measurements EA-06-125-BB-120, a self-temperature compensated Constantan (Ni-Cu alloy) gauge of 0.125-inch active gauge length, 120Ω resistance, bonded to the composite rod with M-Bond 200 cement. For high field strain measurements, a 1-inch (2.54 cm) long piece of the 1/4-inch (6mm) diameter rod with the gauge was mounted in a plexiglass holder between the pole faces of the electromagnet. Magnetic fields to 15.7 kOe were applied parallel to the axis of the short cylinder. A pin inserted in a diametrical hole in the center of the specimen through the plexiglass holder prevented the specimen from touching either pole of the magnet. Strains were read directly on an SR-4 meter with both increasing and decreasing magnetic fields in both directions. Lower field measurements to 300 Oe were made in the solenoid on the same 6-inch (15 cm) long rods used for the B-H determinations.

Previous work using this gauge to measure the magnetostriction of nickel to about 7 kOe(4) had shown no magnetoresistive or magnetostrictive effect of the gauge itself in the magnetic field. Unexpectedly, a large magnetoresistive effect in the gauge was found above about 7 kOe in this work. This effect had never been seen by the gauge manufacturer(10). The magnetoresistance of the gauge manifested itself as an apparent magnetostrictive strain of the same sign (negative) as the nickel or Ni Sm-Fe composite bars. The effect proved to be quite reproducible from gauge-to-gauge. A calibration curve was generated from a gauge cemented to a plexiglass substrate. This curve was then subtracted from those generated for pure nickel and composite specimens. Although this procedure is undesirable and leads to some loss of accuracy and precision, the basic conclusions about the magnetostriction of the composites were not obscured. Subsequent experimentation with other gauges has shown us that the Nichrome (Ni-Cr) alloy is free of all magnetoresistive effects and will be used in the future, although temperature compensation can be a problem with these gauges.

RESULTS

Metallographic Studies of Fe-Sm Alloy Arc-Melted Buttons

Compositions on either side of the $SmFe_2$ composition were melted initially to see what phases would be present in the as-cast condition and after heat treatment. Because of the very high vapor pressure of samarium (200 Torr at the m.p. of Fe), it was anticipated that this element would be lost to some extent, and that the initial charge should therefore contain an excess of samarium. Generally, charges containing 35 at. % Sm were melted. The microstructure of one of these buttons is shown in Figure 3. The as-cast microstructure consists of a white blocky phase, Sm_2Fe_{17}, surrounded by the eutectic. The cooling rate was too fast to form the $SmFe_2$ or $SmFe_3$ phases as called for by the equilibrium phase diagram (Figure 4). Annealing this cast button for 24 hours at 1600°F (871°C) resulted in volatilization of the pure samarium of the eutectic and formation of the $SmFe_2$ compound. The $SmFe_2$ phase is recognizable by its striated appearance as can be seen in the micro of the alloy prepared by A.E. Clark of NOL (Figure 5). The striations on crystallographic planes are thought to be a Widmanstatten precipitate of the $SmFe_3$ phase and can be avoided by more rapid cooling(8).

In Figure 6, the microstructures of a 30 at. % Sm-70 at. % Fe alloy in the as-cast and heat treated condition is shown. The as-cast structure now contains two phases in addition to the eutectic. After the anneal, much of the white phase has disappeared and the striated $SmFe_2$ phase appears. Electron microprobe analysis of this structure (Figure 7) shows the white phase to be Sm_2Fe_{17}, the grey phase to be $SmFe_2$, and the black to be the samarium-rich eutectic. This structure is significant in that it is characteristic of a samarium-lean alloy such as that resulting from excessive samarium loss by volatilization during melting or annealing.

Loss of even more samarium, as simulated in a 25 at. % Sm-75 at. % Fe alloy (Figure 8), results in a structure after the anneal containing none of the $SmFe_2$ phase. The structure is largely $SmFe_3$ plus a small amount of Sm_2Fe_{17} (white phase) and voids from volatilization of the pure samarium of the eutectic.

The Extruded Composites

Mechanical Properties. To the naked eye, bars machined from the composite extrusions were indistinguishable from pure nickel. These bars had been turned on a lathe with no precautions necessary for pyrophoric behavior of chips. Hardnesses on the Rockwell B scale of the four composite rods and the Ni-270 rod are listed in Table I. The dispersed Sm-Fe particles increases the hardness somewhat. After extrusion at 1400°F, the 20% Sm-Fe composite is harder than the 10% composite which is harder than pure nickel.

Tensile properties were determined on a miniature tensile specimen (3/4-inch gauge length, 0.135-inch diameter) machined from the Ni-20 wt. % Sm-Fe composite bar. The 0.2% offset yield strength was 21,000 psi (145 MPa), and the ultimate strength 36,900 psi (254 MPa). Most importantly, the tensile elongation was 3.5% with a reduction in area of 4.5%. The tensile ductility of the Sm-Fe compounds themselves is nil.

Microstructures of the Composite Bars. Photomicrographs of transverse and longitudinal sections of the two 1400°F (760°C) extrusions are shown in Figures 9 and 10. The individual particles withstood a considerable amount of deformation resulting in the elongated particles of the longitudinal section. A large range of particle size is evident. Particle sizes as large as 200 mesh (250μ) to less than the 325 mesh size (<44μ) had been included in the original powder mix. The particles appear to be well bonded to the nickel matrix with only occasional voids at the trailing edges of particles where nickel did not flow in behind.

The particles of the Sm-Fe compounds themselves show a distribution of voids. Some of this undoubtedly derives from the porosity of the original Sm-Fe alloy buttons (see Figure 3). Totally brittle behavior of the Sm-Fe particles would have resulted in breaks with intrusions of nickel. These are only rarely seen. The nickel matrix is completely consolidated.

Some electron probe microanalysis was done to determine the Sm-Fe or Sm-Ni-Fe compounds present in the composite rods following the extrusion operation. The results are summarized in Table II. Scanning electron micros of the particles analyzed are shown in Figure 11. From Table III one notes immediately, that at least in the case of the particles selected, the $SmFe_2$ phase was not found. This is due first to the samarium loss noted above, and secondly to the strong likelihood of a thermal excursion due to adiabatic heating during extrusion to above 900°C (1652°F), the temperature above which the $SmFe_2$ will decompose to form liquid plus the $SmFe_3$ phase (see Figure 4). A slower extrusion speed would minimize this tendency.

A definite zone of reaction of the Sm-Fe particle with the nickel matrix is evident in Figures 10 and 11b in the case of the 20 wt. % Sm-Fe/Ni composite extruded at 1400°F. Similar reaction zones surrounding many of the Sm-Fe particles of the 1200 and 1600°F extrusions were seen in the micrographs of these bars suggesting again considerable heating during extrusion. This zone appears to be $SmNi_3$ (Points 5 and 6, Figure 11b and Table III). The $SmFe_5$ phase does not exist according to Buschow(10), but the equivalent phase does exist in the Ni-Sm and Co-Sm systems. Interestingly, with a small amount of nickel present through diffusion, a phase of the 1-5 stoichiometry was found in the 10% Sm-Fe, 1400°F extrusion.

Magnetic Measurements

Saturation Magnetization. The saturation magnetic moments determined for the starting Sm-Fe powder and the four composite bars are given in Table III. Both the saturation moment σ_s (defined for H = 0) and the moment at 10 kOe (σ_{10}) are listed. These values as well as the slope of the moment-field curve were determined from a linear regression of data measured at magnetic fields ranging between 7.75 and 11.35 kOe.

A sample of $SmFe_2$ prepared by A.E. Clark (NSW) and a nickel pellet (>99.98%Ni) were measured as standards. The magnetic moments at 10 kOe of these two materials are almost equivalent. However the large slope for $SmFe_2$ (1.09 emu/g-kOe) indicates that magnetic saturation has not been achieved for this material at measuring fields up to 11 kOe.

Four samples (3 chunks, one powder each weighing about 0.1 g) of the Sm-Fe alloy prepared at PDMRL were also measured. A wide variation in σ_{10} was observed indicating inhomogeneities in the material. The fact that all of the moments are larger than those found for the Clark material are indicative of samarium loss during preparation. These results are consistent with the metallographic examination discussed earlier. The large slope, independent of particle size, implies that the magnetic hardness arises from magnetocrystalline anisotropy.

The saturation moment, σ_S, of the three Ni-10% Sm-Fe extrusions are all nearly equivalent and slightly larger than the value for pure nickel. Since σ_S and σ_{10} of $SmFe_2$ are both less than the equivalent quantities of pure nickel, it means that the Sm-Fe particles are, on the average, low in samarium.

There is a progressive increase in the slopes with extrusion temperature. It is not known if this reflects the increased reactivity of the nickel matrix and Sm-Fe alloy particles with temperature. Doubling the Sm-Fe loading resulted in a modest increase in σ_S and a doubling of the slopes. Generally, compounds other than the $SmFe_2$ would be expected to have very high magnetocrystalline anisotropies and thus higher slopes in this measurement because of their non-cubic crystal structures.

The composite materials can be said to behave as a simple mixture of magnetic phases - one of which is magnetically hard.

<u>B-H Curves</u>. The primary magnetization curves for a 6-inch (15 cm) long bar of the Ni-20% Sm-Fe composite is shown in Figure 12. The composite material is considerably harder than the pure nickel (Ni-270) standard. At 300 Oe applied field, the composite material has attained an induction level of 4500 gauss while the nickel standard is approaching technical saturation.

<u>Magnetostriction Measurements</u>

<u>High Field Strain Measurements</u>. The magnetostrictive strain of samples taken from the four extruded bars was measured as a function of applied field (to 15.7 kOe) by the strain gauge technique described earlier. Direct interpretation of these results is confounded by a magnetostrictive response of the strain gauges employed. Nevertheless, a procedure was devised to permit extraction of the pertinent data.

A calibration curve for the Micro-Measurement Constantan gauges was measured and the result is shown in

Figure 13. In this experiment, the strain gauge was cemented to a plexiglass rod of approximately the same dimensions as the extruded Ni Sm-Fe composites. For each strain measurement, the gauge was first nulled, then the magnetizing current set at the desired level and the strain read ($\pm 2\mu$ in/in), finally the current was shut off to ascertain a return to the null position. This procedure minimized instrumental drift caused by the high heat capacity and high thermal expansivity of the plexiglass. The observed contraction grows monotonically - although not linearly - with magnetizing field and reaches a value of -24.5 μ in/in at 15.7 kOe.

The magnetostrictive strain of a sample of pure nickel (Ni-270) was also measured to check the experimental technique. These data are shown in Figure 14. A summary of the data are also provided in Table IV. Strain measurements were recorded as the magnetizing field was increased (U) and then decreased (D). Little instrumental drift was encountered with the metallic samples so that the repeated null check was not required. The average strain readings, $[U(I) + D(I)]/2$, were reduced by the gauge contribution and both values plotted on Figure 14. The net magnetostrictive strain varies between 33 and 38 μ in/in with the larger values predominating at the higher fields. In view of the large corrections needed to arrive at these data, refined analyses are not believed warranted. The expected behavior for a pure nickel specimen is to reach a saturation strain value of -37 μ in/in at approximately 1 kOe and exhibit a further small contraction with increasing field due to forced magnetization. An average strain of -35 μ in/in was computed from all of the experimental data - independent of field. This agreement verifies the experimental technique and provides a standard for comparison with the Ni/Sm-Fe composite materials.

The magnetostrictive strain measurements of the 20% Sm-Fe sample are summarized in Figure 15. Both sets of strain values as tabulated in Table IV are plotted to indicate the degree of magnetic/magnetostrictive hysteresis encountered. Although Sm-Fe compounds are known to possess high magnetocrystalline anisotropies(5), little if any magnetostrictive hysteresis was encountered for fields up to 15.7 kOe. The strain values were therefore averaged at each field level and then reduced by the instrumental contribution. The net magnetostrictive strain varied from -37 to -42.5 μ in/in. An average strain of -39.3 μ in/in was computed from all of the experimental data. This value is 12% larger than that obtained for the pure nickel samples.

Similar strain measurements for the 10% Sm-Fe composites extruded at 1600, 1400 and 1200°F are summarized in Figures 16, 17 and 18 respectively. An average strain of -41.9 μ in/in (19.7% larger than the Ni-270 bar) was obtained for the 1600°F extrusion. The 1400°F extrusion gave an average value of -42.5 μ in/in (21.4%). Magnetostrictive strain measurements on the 1200°F sample are not consistent with the other data reported here and a faulty strain gauge is suspected.

In summary, the high field strain measurements on the Ni/Sm-Fe composites show a modest (12 to 20%) increase in strain over the Ni-270 control. Little change in the shape of the strain-field curves was noted.

Low Field Strain Measurements. Strain measurements were also obtained on a 6-inch long by 0.25-inch diameter rod machined from the Ni/20% Sm-Fe extrusion. The same type of strain gauge was employed and the magnetizing field was generated by a multilayered solenoid. A 5.5-inch long rod of Ni-270 was also measured as a control. As before, little magnetic/magnetostriction hysteresis was encountered and no instrumental correction is required at the low field levels employed (to ∿300 Oe). The strain measurements are summarized in Figure 19. These curves are similar to the induction curves shown in Figure 12. The Ni-270 curve is approaching saturation while the magnetically harder Ni/20% Sm-Fe sample is at only 60% of its saturation strain at 300 Oe.

The magnetostrictive strain of Ni-270 measured in the interval $150 \leq H \leq 300$ Oe is slightly larger than the values reported in Figure 14 and measured at fields to 15 kOe. This difference (approximately 4 μ in/in) is believed to arise mainly from the instrumental correction required for the high field measurements.

Magnetomechanical Coupling. Electrical impedance values measured as a function of excitation frequency were used to determine coupling of both the Ni-20% Sm-Fe and Ni-270 rods. These rods were driven in the length mode at frequencies near the fundamental. Two bias levels (85 and 170 Oe) were examined for the composite while the Ni-270 control was measured at 85 Oe only. In all these cases, the impedance loops were small and poorly defined. An impedance loop for the composite is shown in Figure 20. Mechanical resonance occurs at approximately 13,800 Hz. At frequencies well above and below resonance, a large loss angle is noted (approximately 50° from the X-axis in this case). This was observed for both materials and is indicative of electrical shielding by eddy currents in these highly conductive materials. Consequently the magnetomechanical coupling was low (less than 5%) and detailed measurements were not attempted.

Mechanical resonance of the Ni-270 rod was at approximately 17,725 Hz. Adjusting this value for the difference in length of the two rods gives a resonant frequency of 16,250 Hz. Resonance in the Ni/20% Sm-Fe rod occurred at 84.9% of this value.

DISCUSSION

The composites of this study proved to have only a very small (12 to 20%) increase in magnetostrictive strain compared to the pure nickel matrix material. The basic reason for this result relates to the composition of the Sm-Fe component of the composite. The particles are largely the Sm_2Fe_{17} and $SmFe_3$ compounds rather than the $SmFe_2$. These higher iron compounds found to be present in the metallographic study have lower magnetostrictions and much larger magnetocrystalline anisotropies. In addition, a good deal of eutectic material was present in the Sm-Fe particles at various stages in the processing. Volatilization of the pure samarium of the eutectic leads to voids. The voids prevent coupling of the magnetostrictive strain to the nickel matrix.

A number of improvements to the procedures used in this first attempt at fabricating a Metal/RE-Fe composite are as follows:

1. Use of induction melting of a larger ingot of the $SmFe_2$ compound to minimize the surface-to-volume ratio and thus the samarium loss. Good composition control will result after the homogenization anneal in largely the $SmFe_2$ with a minimum of the other phases. It is very important to avoid residual eutectic.

2. Lower extrusion speeds will avoid overheating and decomposition of the $SmFe_2$ phase.

3. The smallest portion of the $SmFe_2$ particle size distribution should be eliminated. These particles, according to the electron microprobe analysis, are converted to a Ni-Sm compound. The smallest particle must be several times the reaction zone thickness which is about 3μ in the 1400°F extrusions.

4. Alignment of the $SmFe_2$ particles in the powder mix prior to extrusion might result in the easy magnetization direction

<111> parallel to the bar axis. Thus lowering the magnetic fields necessary to magnetize the $SmFe_2$ component.

5. Substitution of a ternary or quaternary RE-Fe compound known to have low anisotropy should also result in lower applied fields. If the $Dy_{0.7}Tb_{0.3}Fe_2$ compound or other compounds with positive magnetostriction were chosen, a matrix also having positive magnetostriction such as a Ni-Fe or Fe-Co alloy matrix should be used. The use of $Sm_{0.88}Dy_{0.12}Fe_2$ in a pure nickel matrix should be attempted.

RECORDS

Experimental data, photos, and other pertinent information in connection with the performance of the experimental portion of this research project are contained in Experimental Record Book 2727, pages 1-85, on file at the Paul D. Merica Research Laboratory of The International Nickel Company, Inc., Sterling Forest, Suffern, NY 10901.

D.T. Peters — E.L. Huston

REFERENCES

1. A.E. Clark and H.S. Belson, 17th Conference on Magnetism and Magnetic Materials, Chicago, IL, Nov. 1971. See AIP Conf. Proc., 5, (1972), p. 1498.

2. N.C. Koon, A.I. Schindler and F.L. Carter, Phys. Letters, 37A, (1971), p. 413.

3. A.E. Clark and H.S. Belson, Phys. Rev., B5, (1972), p. 3642; also IEEE Trans. Mag. MAG-8, (1972), p. 477.

4. E.L. Huston, D.T. Peters and G.D. Sandrock, IEEE Trans. Mag., MAG-9, (1973), p. 636.

5. A.E. Clark, H.S. Belson and N. Tamagawa, Phys. Letters, 42A, (1972), p. 749.

6. C.M. Williams and N.C. Koon, AIP Conf. Proc., 18, (1973), p. 1247.

7. A.E. Clark, AIP Conf. Proce., 18, (1973), p. 1015.

8. Private communication with A.E. Clark.

9. R.M. Bozorth, H.J. Williams and D.E. Walsh, Phys. Rev., 103, (1956), p. 572.

10. Private communication with James Weidner of Micro-Measurements, Romulus, MI.

11. K.H.J. Buschow, J. Less-Common Metals, 25, (1971), p. 131.

TABLE I

HARDNESS OF EXTRUDED Ni Sm-Fe RODS

Wt. % Sm-Fe	Extrusion Temperature (°F)	R_B Hardness
10	1200	76.4
10	1400	77.5
10	1600	69.0
20	1400	83.6

Ni-270 annealed 1 Hr/1500°F (816°C), R_B 32.9.

TABLE II

ELECTRON PROBE MICROANALYSIS OF
Sm-Fe PARTICLES IN EXTRUDED COMPOSITE RODS

Specimen	Area*	Analysis (At. %) Fe	Sm	Ni	Compound
10 Wt. %Sm-Fe Extruded at 1200°F *See Figure 11a	1	89.40	10.14	0.44	Sm_2Fe_{17}
	2	89.21	10.10	0.68	Sm_2Fe_{17}
	3	72.91	25.00	2.07	$SmFe_3$
	4	72.44	24.90	2.64	$SmFe_3$
	5	72.17	22.62	5.19	--
	6	88.22	9.68	2.08	--
	7	0.26	0.00	99.73	Ni Matrix
10 Wt. %Sm-Fe Extruded at 1400°F *See Figure 11b	1	73.85	24.75	1.39	$SmFe_3$
	2	74.33	24.26	1.39	$SmFe_3$
	3	82.83	14.85	2.30	$Sm(Fe,Ni)_5$?
	4	84.71	14.10	1.18	$Sm(Fe,Ni)_5$?
	5	0.91	25.62	73.45	$SmNi_3$
	6	1.04	25.77	73.17	$SmNi_3$
	7	61.50	15.95	22.54	$Sm(Fe,Ni)_5$
	8	0.0	0.0	100.00	Ni Matrix

TABLE III

SATURATION MAGNETIC MOMENT MEASUREMENTS OF THE Ni Sm-Fe COMPOSITE MATERIALS

Sample		(emu/g) σ_s	σ_{10}	Slope (emu/g-kOe)
$SmFe_2$	(A.E. Clark)	41.1	52.1	1.096
Sm-Fe	Chunk #1	46.7	58.2	1.147
Sm-Fe	Chunk #2	137.6	147.5	0.994
Sm-Fe	Chunk #3	43.3	57.8	1.450
Sm-Fe	Fines	74.0	80.4	0.641
Ni Pellet		54.8	55.16	0.040
Ni-10%Sm-Fe	1200°F	54.6	56.1	0.148
	1400°F	55.2	56.8	0.160
	1600°F	55.2	57.8	0.263
Ni-20%Sm-Fe	1400°F	56.4	56.4	0.294

TABLE IV

MAGNETOSTRICTIVE STRAIN DATA FOR Ni-270 SPECIMEN

Gauge Calibration Curve (Figure 13)

H (kOe)	Strain (μ in/in) Run 1	Run 2	Avg.
0	0	0	0
1.93	0	0	0
3.85	3	1.5	2.25
5.87	5	3	4
7.70	5.5	5.5	5.5
9.50	10.0	10	10
11.3	13.5	13	13.25
12.7	17.5	15	16.25
14.0	20	19	19.5
15.0	22	22.5	22.25
15.7	24	25	24.5

Ni-270 (Figure 14)

H (kOe)	Strain (μ in/in) U	D	Avg.	Net
0	0	0	0	0
1.93	35	33	34	34
3.85	36	35	35.5	33.25
5.87	40	38	39	35
7.70	41	40	40.5	35
9.50	44	42	43	33
11.3	50	45	47.5	34.25
12.7	52	51	51.5	35.25
14.0	55	56	55.5	36
15.0	60	60	60	37.75
15.7	61	61	61	36.5

TABLE IV (CONTINUED)

20%SmFe (Figure 15)

H (kOe)	Strain (μ in/in) U	D	Avg.	Net
0	0	1	3	
1.93	39	37	38	38
3.85	39	39	39	36.75
5.87	43	42	42.5	38.5
7.70	44	44	44	38.5
9.50	48	48	48	38
11.3	53	51	52	38.75
12.7	56	55	55.5	39.25
14.0	62	59	60.5	41
15.0	65	63	64	41.75
15.7	67	67	67	42.5

10%SmFe, 1600°F (Figure 16)

H (kOe)	Strain (μ in/in) U	D	Avg.	Net
0	0	-1		0
1.93	40	42	41	41
3.85	43	44	43.5	41.25
5.87	44	46	45	41
7.70	46	48	47	41.5
9.50	49	52	50.5	40.5
11.3	53	54	53.5	40.25
12.7	59	58	58.5	42.25
14.0	62	62	62	42.5
15.0	66	65	65.5	43.25
15.7	70	70	70	45.5

TABLE IV (CONTINUED)

10%SmFe, 1400°F (Figure 17)

H (kOe)	Strain (μ in/in) U	D	Avg.	Net
0	0	1		0
1.93	39	42	40.5	40.5
3.85	43	44	43.5	41.25
5.87	45	46	45.5	41.5
7.70	46	48	47	41.5
9.50	48	51	49.5	39.5
11.3	53	55	54	40.75
12.7	63	59	61	44.75
14.0	66	62	64	44.5
15.0	69	64	66.5	44.25
15.7	71	71	71	46.5

10%SmFe, 1200°F (Figure 18)

H (kOe)	Strain (μ in/in) U	D	Avg.	Net
0	0	--		0
1.93	34	35	34.5	34.5
3.85	38	37	37.5	35.25
5.87	38	39	38.5	34.5
7.70	39	39	39	33.5
9.50	40	40	40	30
11.3	42	43	42.5	29.25
12.7	43	44	43.5	27.25
14.0	45	46	45.5	26
15.0	49	49	49	26.25
15.7	51	51	51	26.5

TABLE IV (CONTINUED)

(Figure 19)

H (kOe)	Ni-20%SmFe Strain (μ in/in) U	D	Avg.	Ni-270 Strain (μ in/in) U	D	Avg.
0	0	0	0	0	0	0
28.3	3	4	3.5	12	10	11
56.6	8	11	9.5	23	23	23
84.9	15	13	14	28	29	28.5
113.2	16	14	15	35	30	32.5
141.5	17	15	16	36	34	35
169.8	20	16	18	36	34	35
198.1	20	20	20	36	36	36
226.4	21	20	20.5	38	36	37
254.7	23	21	22	39	36	37.5
283.0	23	22	22.5	39	36	37.5
311.3	26	26	26	39	39	39

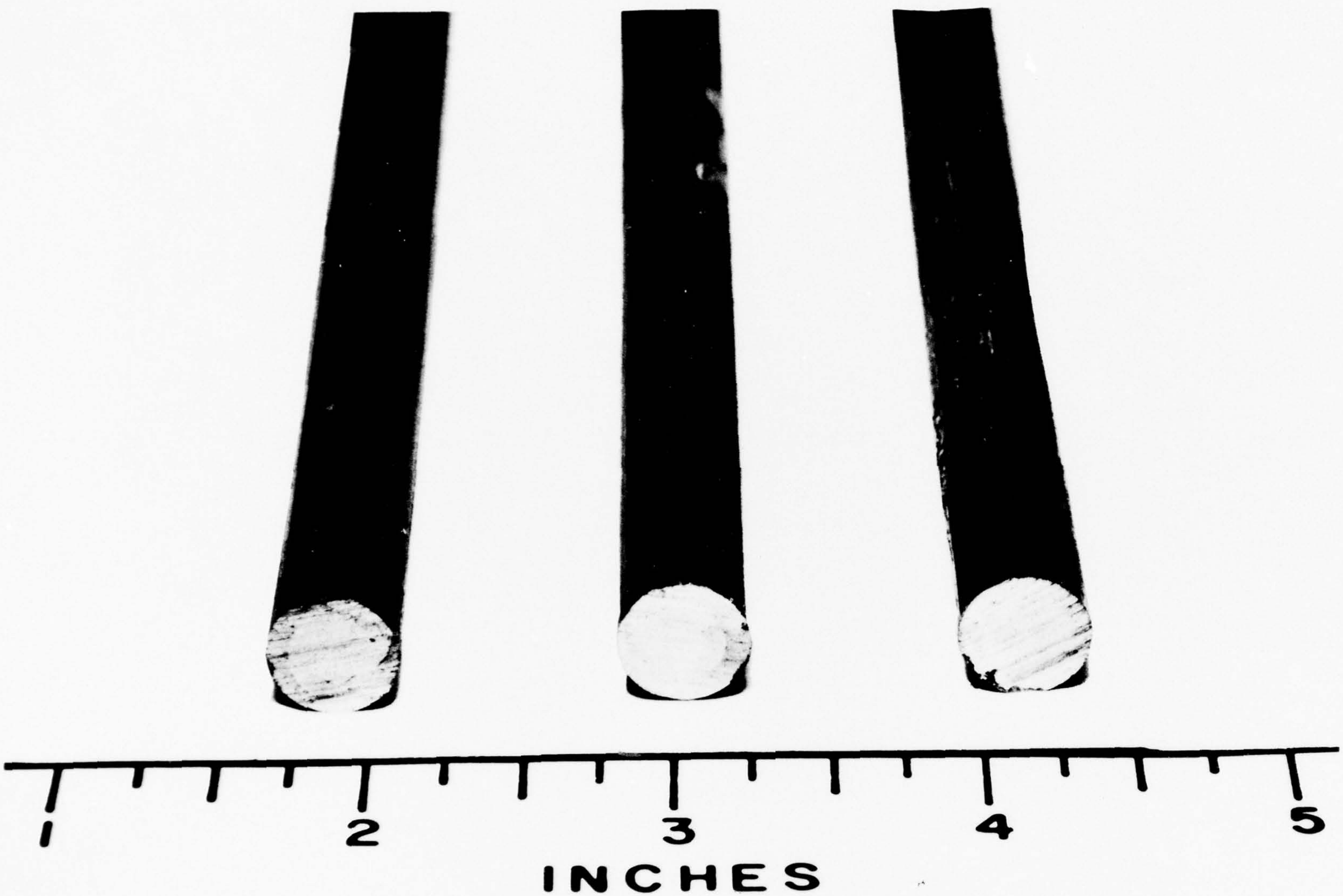

P.N. 2-58445

1X

FIGURE 1

Ni-10%Sm-Fe COMPOSITE BAR STOCK IN COPPER CANNING MATERIAL AFTER EXTRUSION AT 1200°F. EXTRUDED BAR HAS BEEN CUT INTO THREE EQUAL LENGTHS AND HEAD AND TAIL PORTIONS DISCARDED.

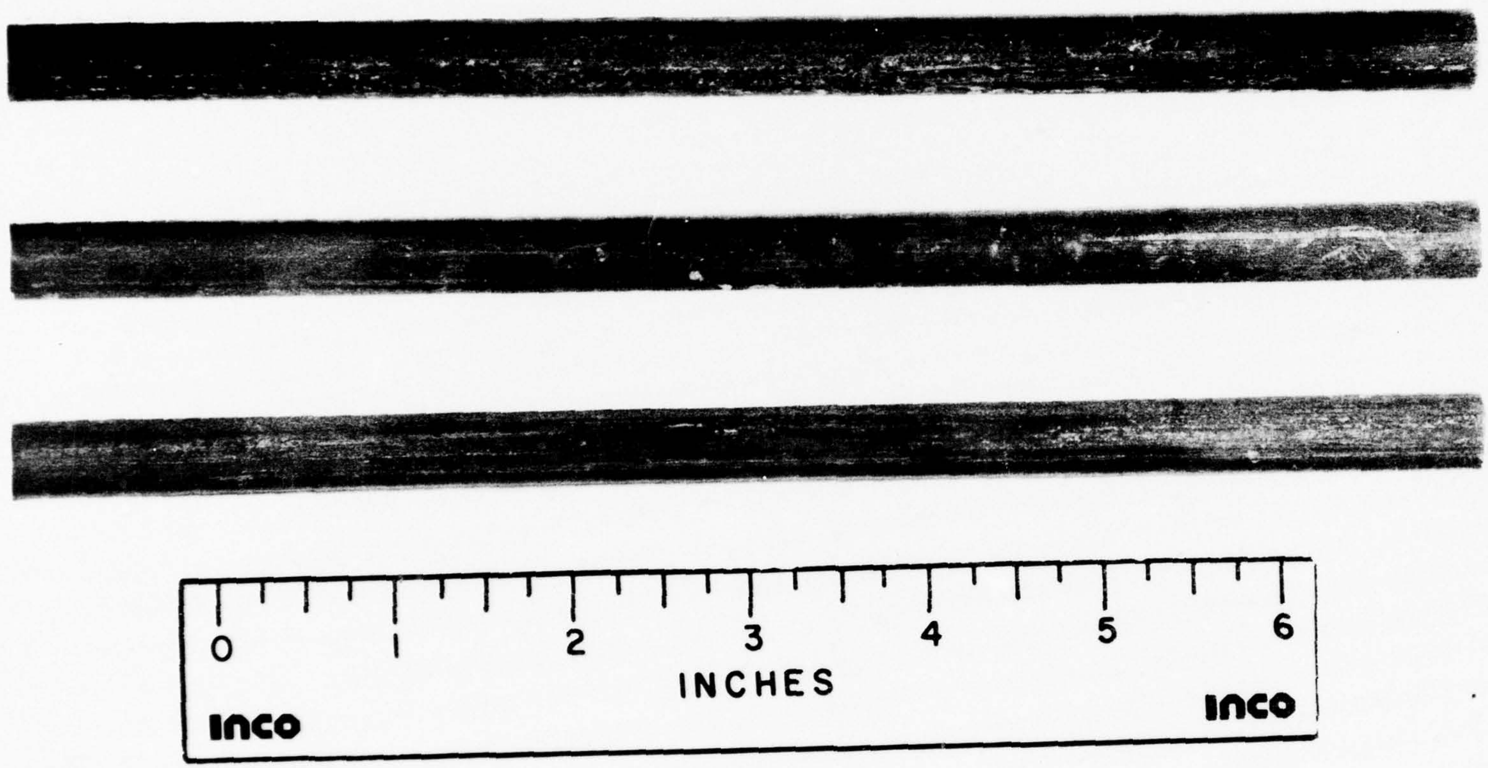

P.N. 2-58448

FIGURE 2

Ni-10%Sm-Fe COMPOSITE BAR STOCK IN COPPER CANNING MATERIAL AFTER EXTRUSION AT 1600°F. THE COPPER JACKET IS VISIBLE ON THE CUT ENDS OF THIS 2X MACROGRAPH.

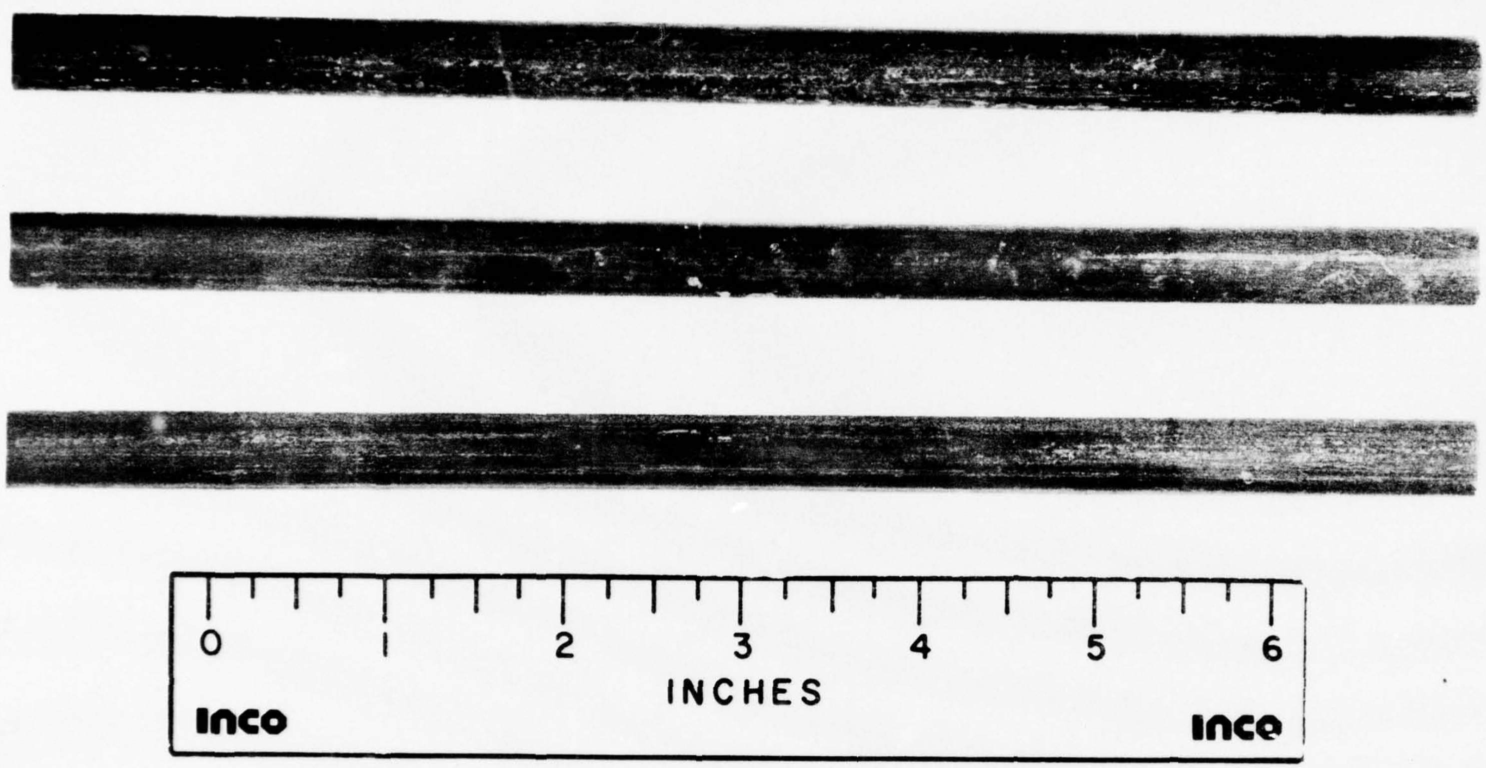

P.N. 2-58448

FIGURE 2

Ni-10%Sm-Fe COMPOSITE BAR STOCK IN COPPER CANNING MATERIAL AFTER EXTRUSION AT 1600°F. THE COPPER JACKET IS VISIBLE ON THE CUT ENDS OF THIS 2X MACROGRAPH.

P.N. 51423 200X

(a) As-Cast

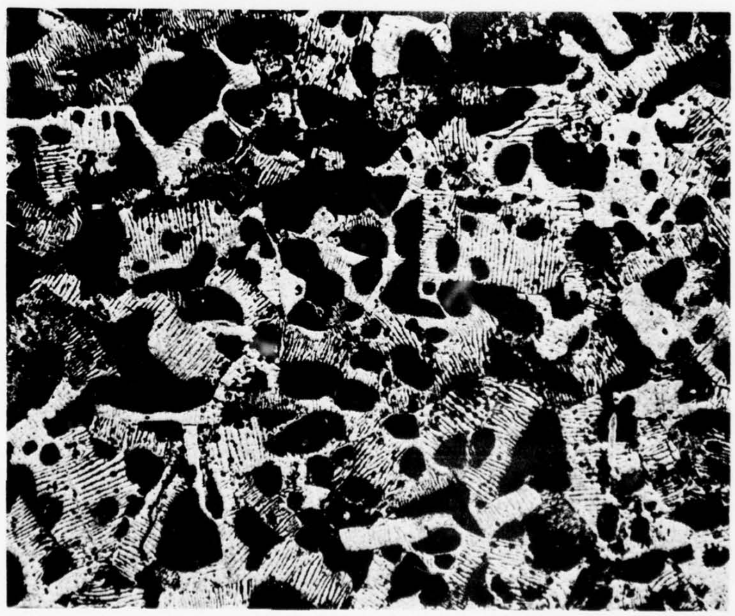

P.N. 51495 200X

(b) 24 Hrs/850°C (1562°F)

FIGURE 3

PHOTOMICROGRAPHS OF 35 AT. % Sm-65 AT. % Fe
ALLOY ARC MELTED BUTTON

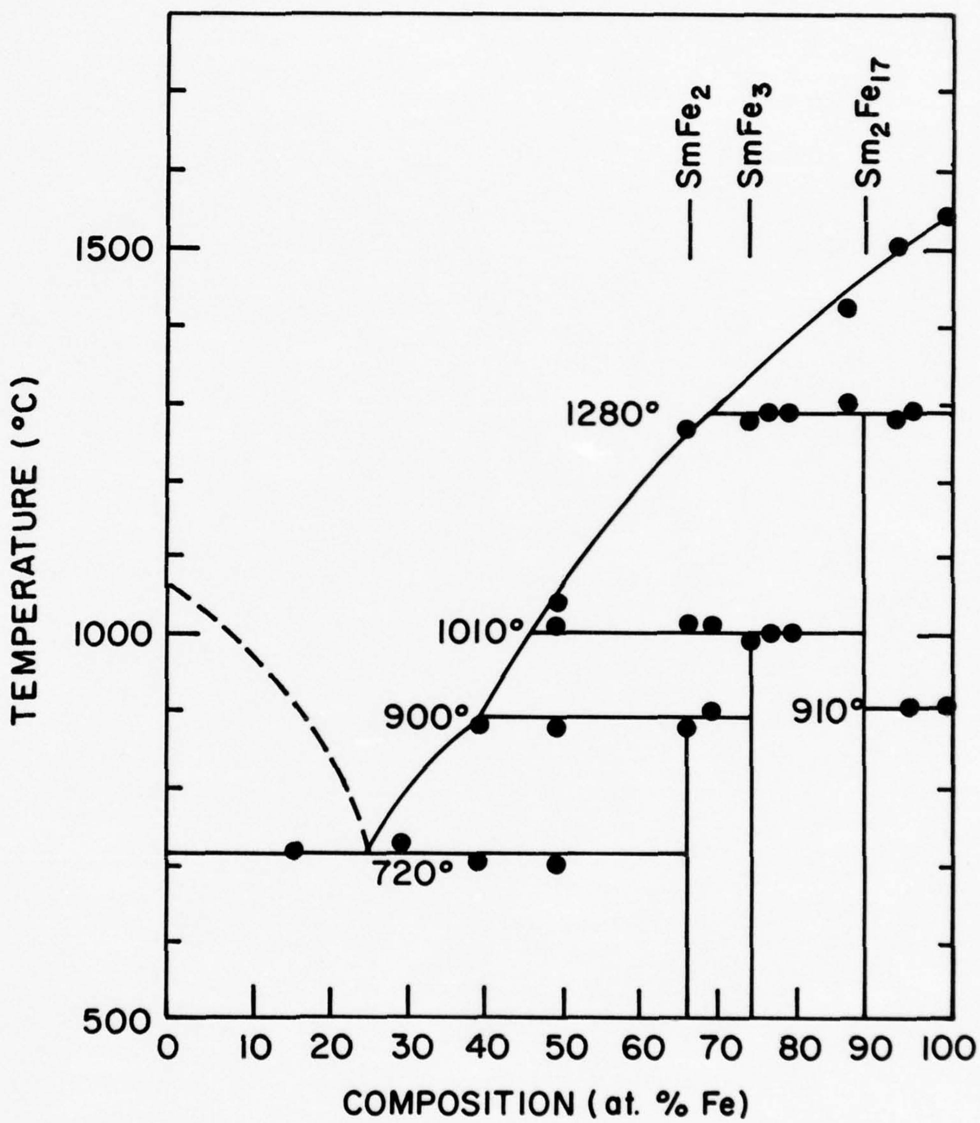

<u>FIGURE 4</u> - Sm-Fe BINARY PHASE DIAGRAM (AFTER BUSCHOW - REF. 11).

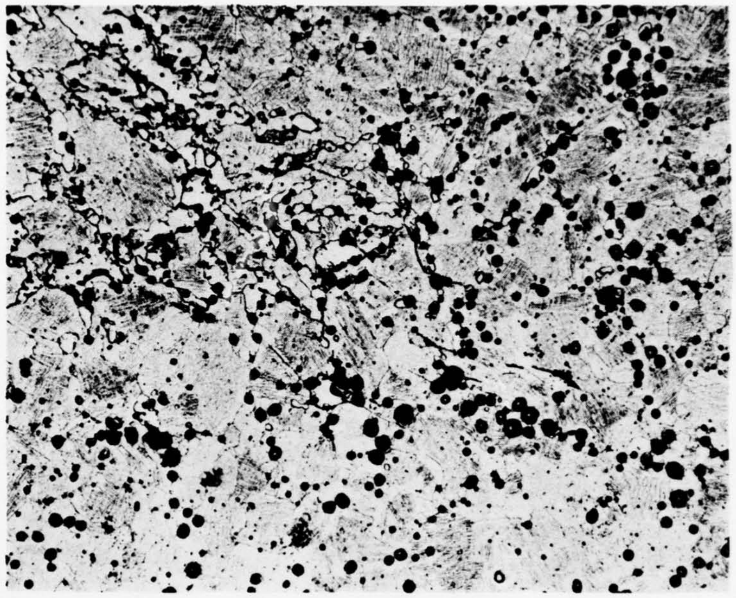

P.N. 49134 100X
(a) Center of Bar

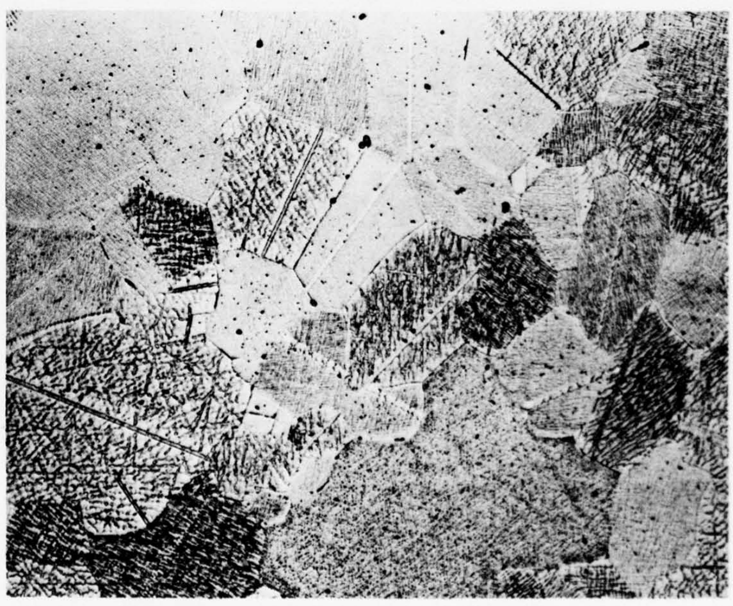

P.N. 49135 100X
(b) Near Outer Edge of Bar

FIGURE 5

PHOTOMICROGRAPHS OF $SmFe_2$ SAMPLE PROVIDED BY A.E. CLARK. CAST AND ANNEALED 30 DAYS AT 850°C.

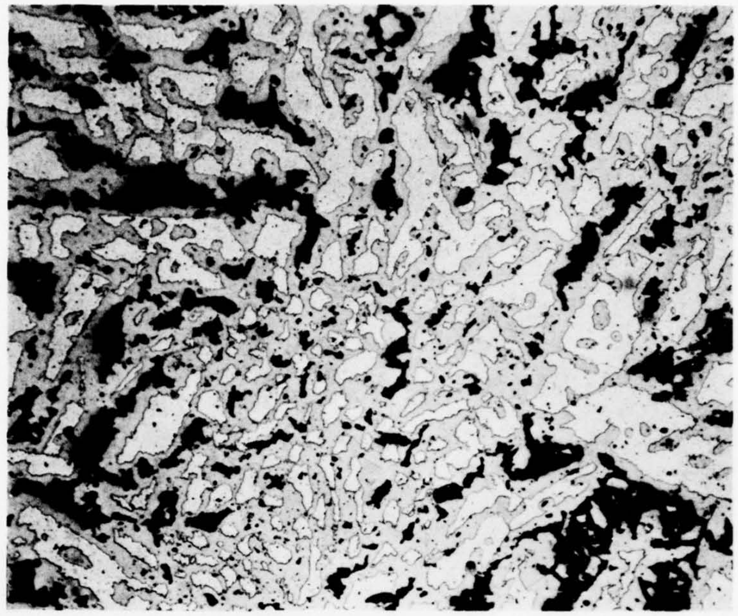

P.N. 51427 200X

(a) As-Cast

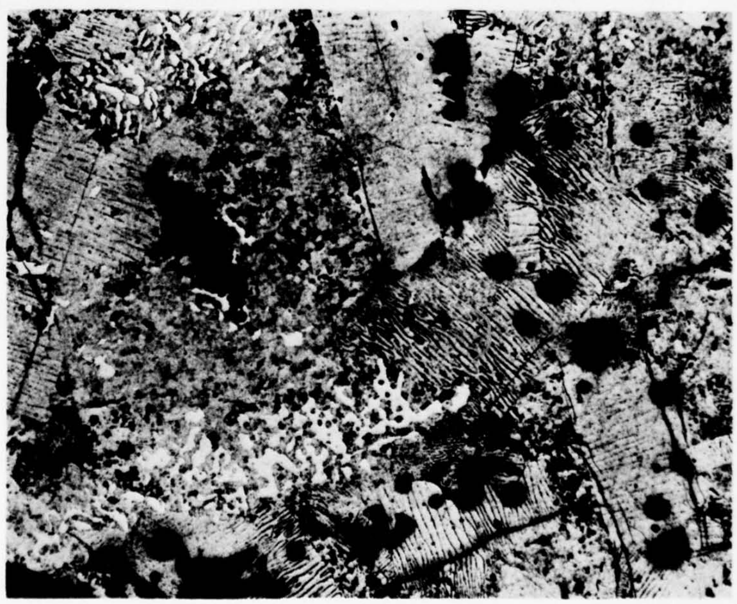

P.N. 51498 100X

(b) 24 Hrs/850°C (1562°F)

FIGURE 6

PHOTOMICROGRAPHS OF 30 AT. % Sm-70 AT. % Fe ALLOY ARC MELTED BUTTON

	Point	Element	Weight Percent	Atomic Percent
White Phase	1.	Sm Lα	24.76	11.13
		Fe Kα	73.41	88.86
Sm_2Fe_{17}	2.	Sm Lα	24.23	10.92
		Fe Kα	73.41	89.07
Grey Phase	3.	Sm Lα	56.77	33.35
		Fe Kα	42.13	66.64
$SmFe_2$	4.	Sm Lα	55.87	32.08
		Fe Kα	43.93	67.91
Black Phase	5.	Sm Lα	97.73	97.50
		Fe Kα	0.92	2.49
Eutectic	6.	Sm Lα	61.71	40.56
		Fe Kα	33.58	59.43

Sm determined relative to a standard of $SmFe_2$
Fe determined relative to a standard of $SmFe_2$

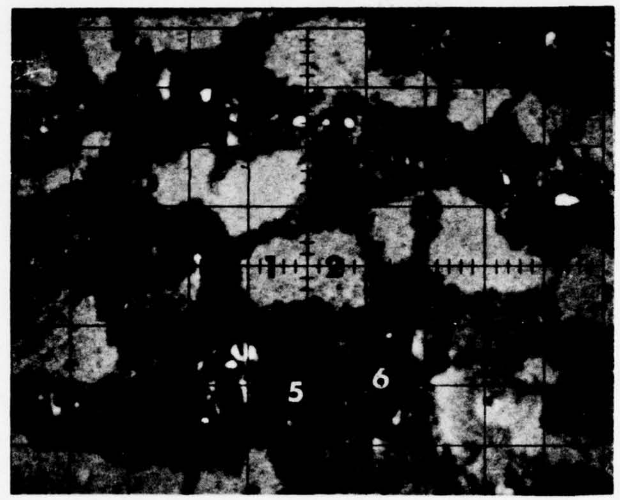

1304-71 SEM (RI) 750X

FIGURE 7

ELECTRON MICROPROBE ANALYSIS OF THE ANNEALED 30 AT. % Sm-70 AT. % Fe ALLOY

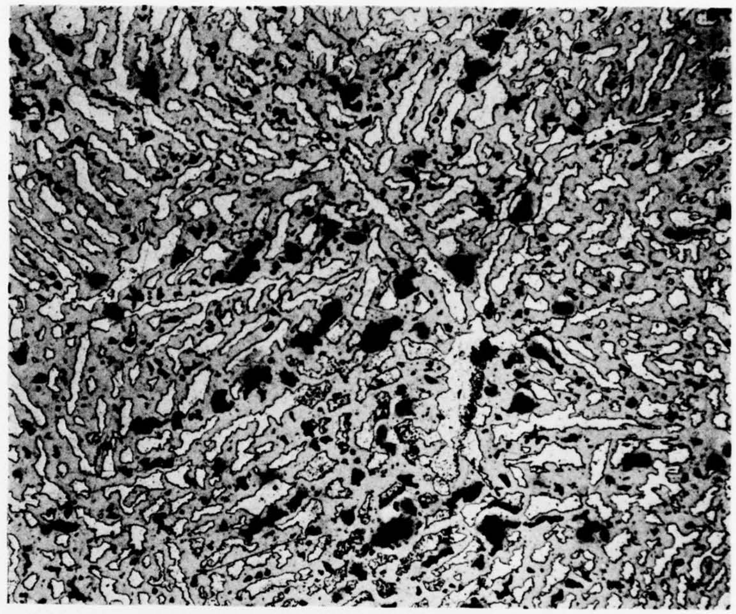

P.N. 51431 200X

(a) As-Cast

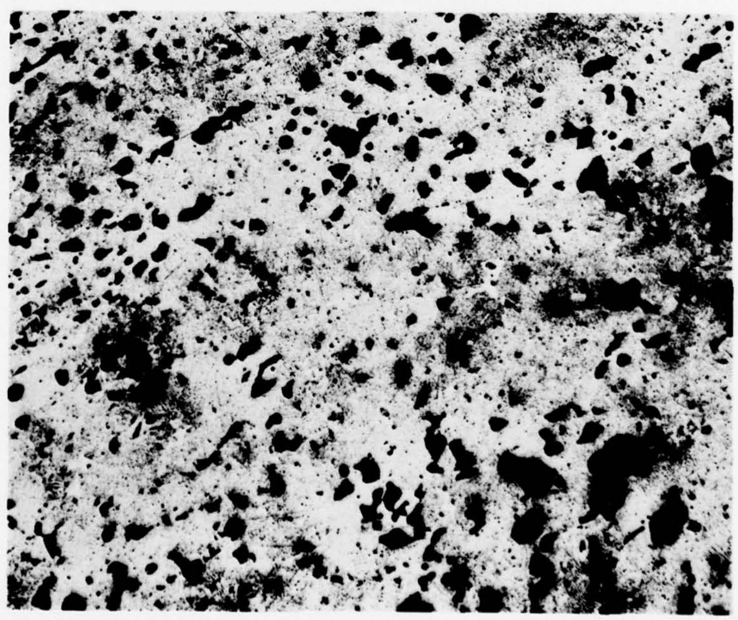

P.N. 51500 100X

(b) 24 Hrs/850°C (1562°F)

FIGURE 8

PHOTOMICROGRAPHS OF 25 AT. % Sm-75 AT. % Fe ALLOY ARC MELTED BUTTON

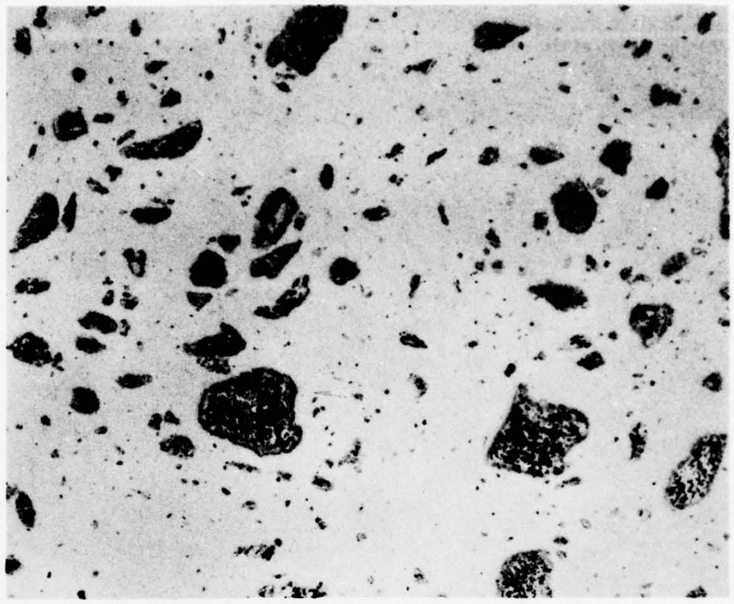

P.N. 58483 100X
(a) Transverse Section

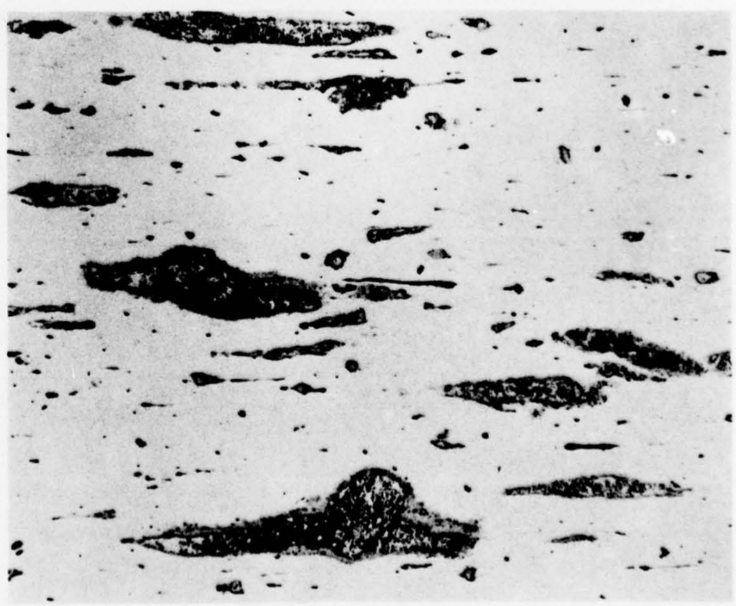

P.N. 58482 100X
(b) Longitudinal Section

FIGURE 9

PHOTOMICROGRAPHS OF THE Ni-10 WT. % Sm-Fe COMPOSITE AS EXTRUDED AT 1400°F (760°C)

UNETCHED

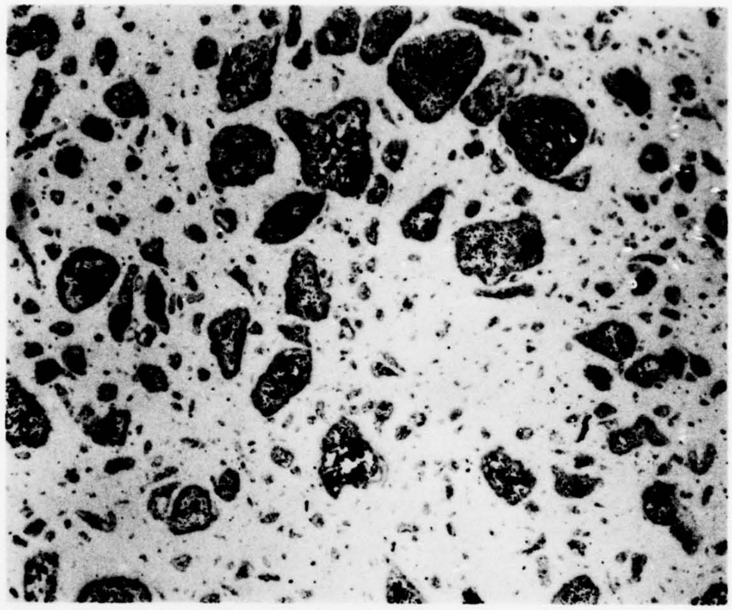

P.N. 58489 100X

(a) Transverse Section

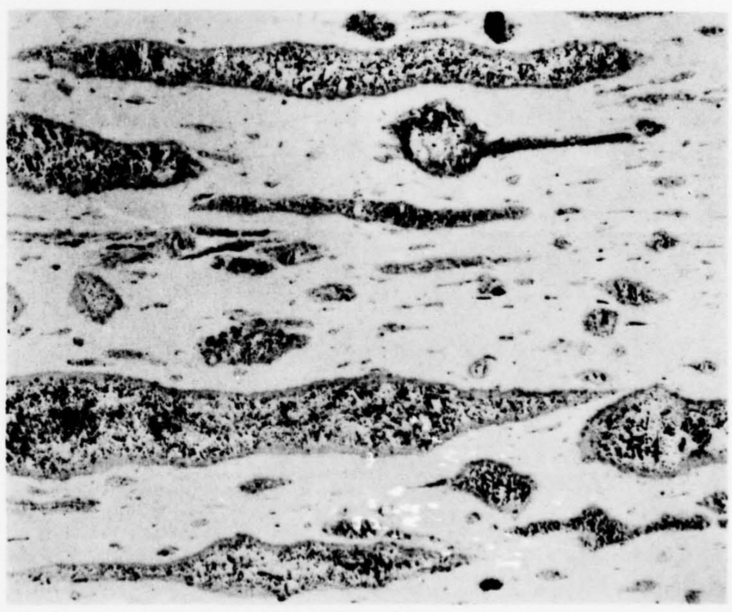

P.N. 58488 100X

(b) Longitudinal Section

FIGURE 10

PHOTOMICROGRAPHS OF THE Ni-20 WT. % Sm-Fe COMPOSITE AS EXTRUDED AT 1400°F (760°C)

UNETCHED

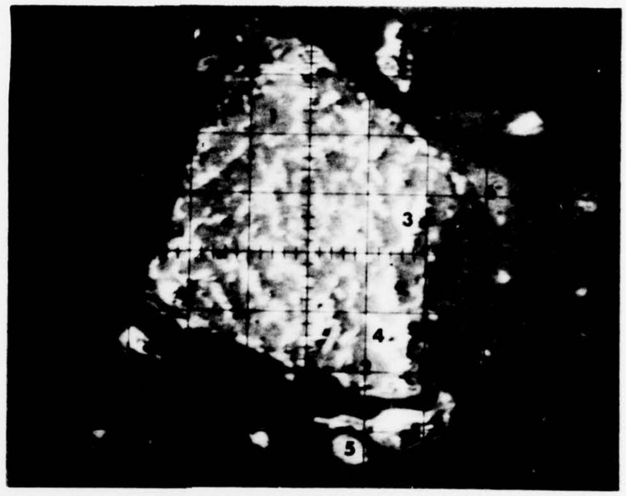

1369-11 330X

(a) Extruded at 1200°F

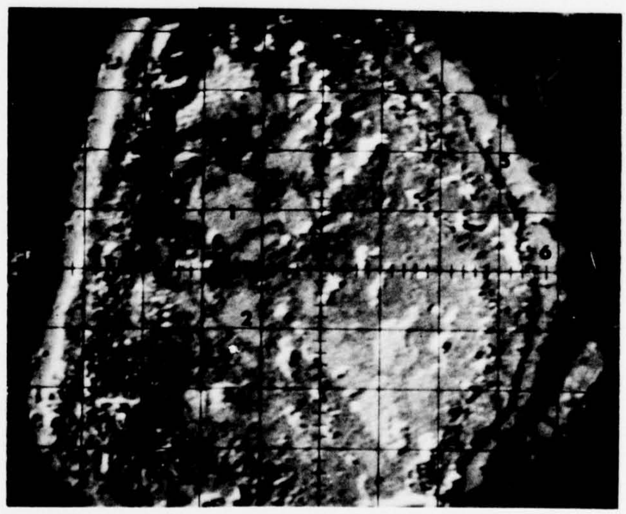

1369-21 330X

(b) Extruded at 1400°F

FIGURE 11

SCANNING ELECTRON MICROGRAPHS (SPECIMEN CURRENT) OF TYPICAL Sm-Fe PARTICLES IN THE 10 WT. % Sm-Fe/Ni EXTRUDED COMPOSITE RODS

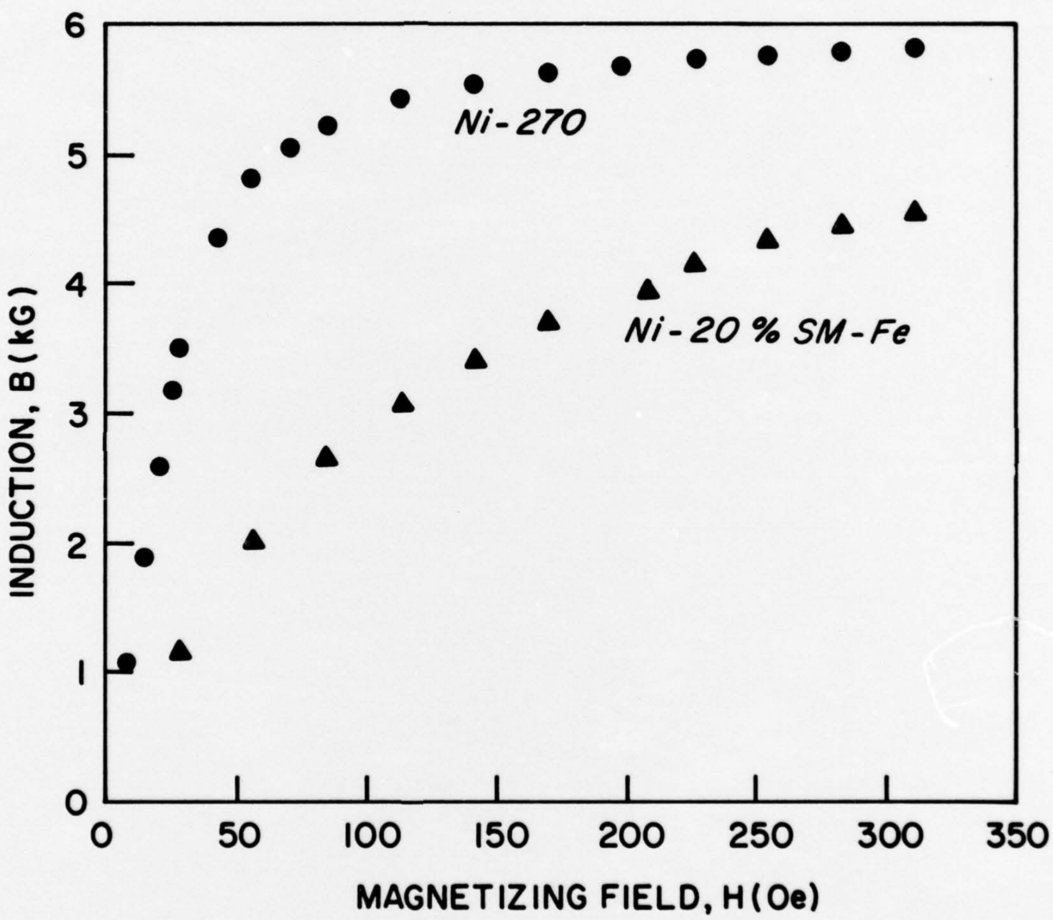

FIGURE 12 - PRIMARY MAGNETIZATION CURVE FOR LONG (~5.5") BARS OF Ni-270 AND THE Ni-20% Sm-Fe COMPOSITE.

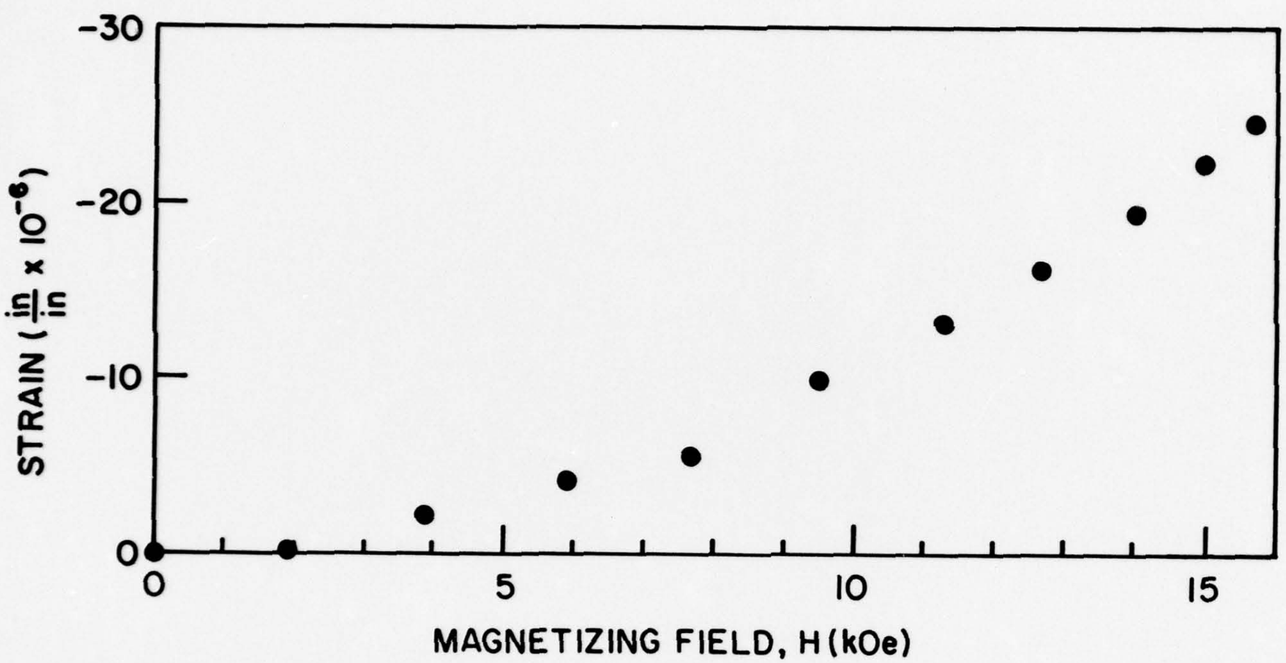

FIGURE 13 - CALIBRATION CURVE FOR THE MICRO-MEASUREMENT CONSTANTAN ALLOY STRAIN GAUGE.
EA-06-125-BB-120 MOUNTED ON PLEXIGLAS

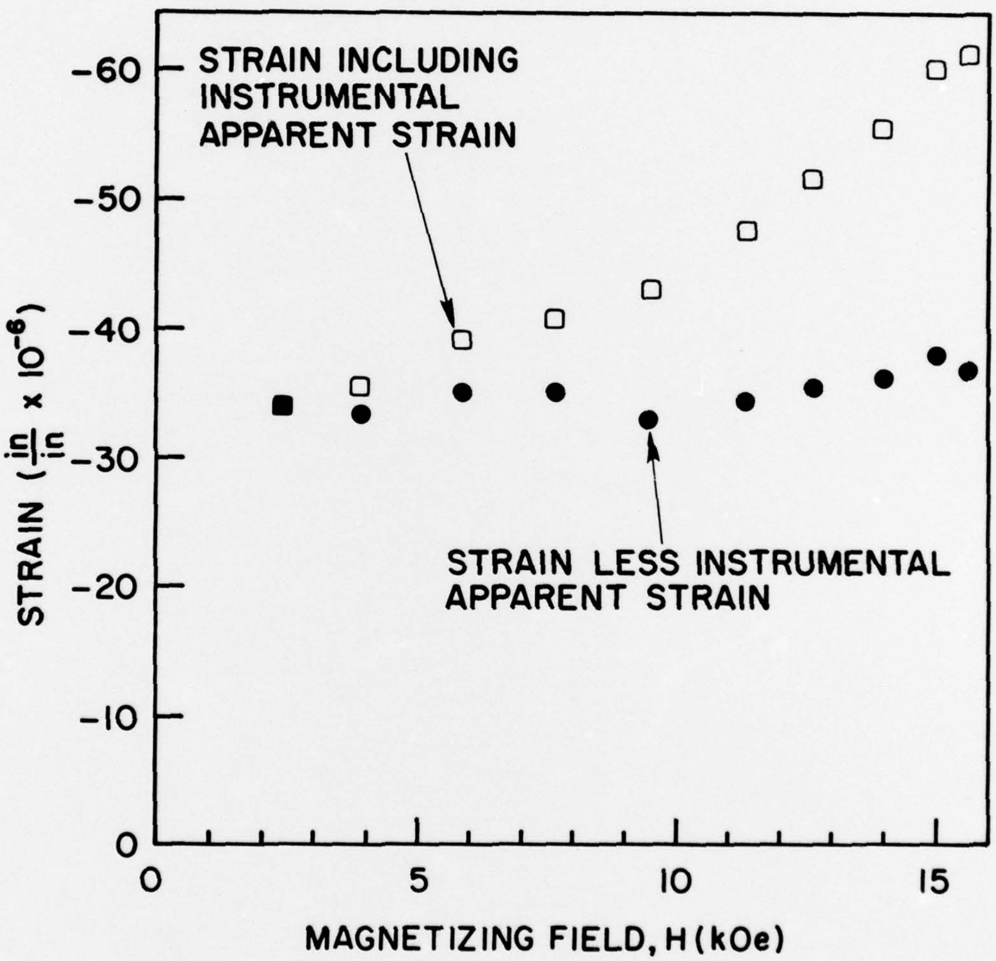

FIGURE 14 - STRAIN AS A FUNCTION OF APPLIED FIELD FOR Ni-270.

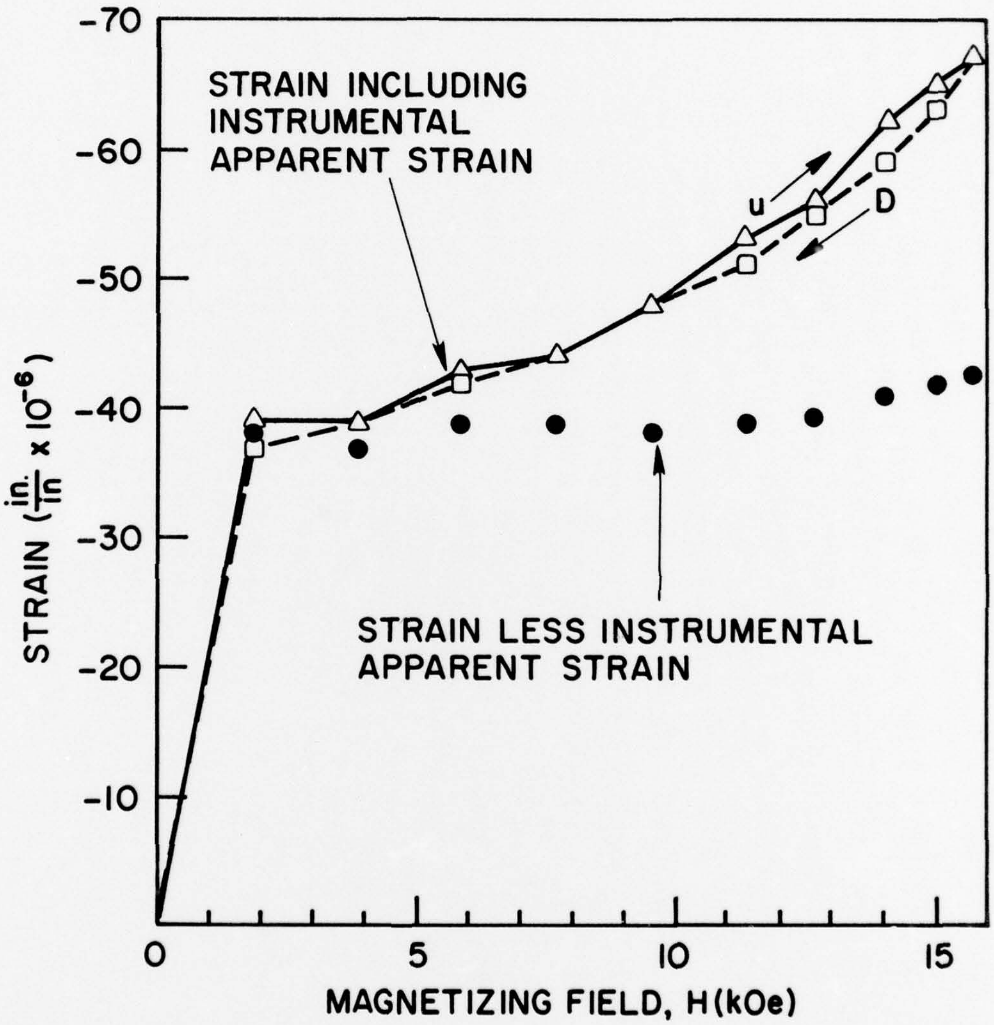

FIGURE 15 - STRAIN AS A FUNCTION OF APPLIED FIELD FOR THE Ni/20% Sm-Fe COMPOSITE EXTRUDED AT 1400°F.

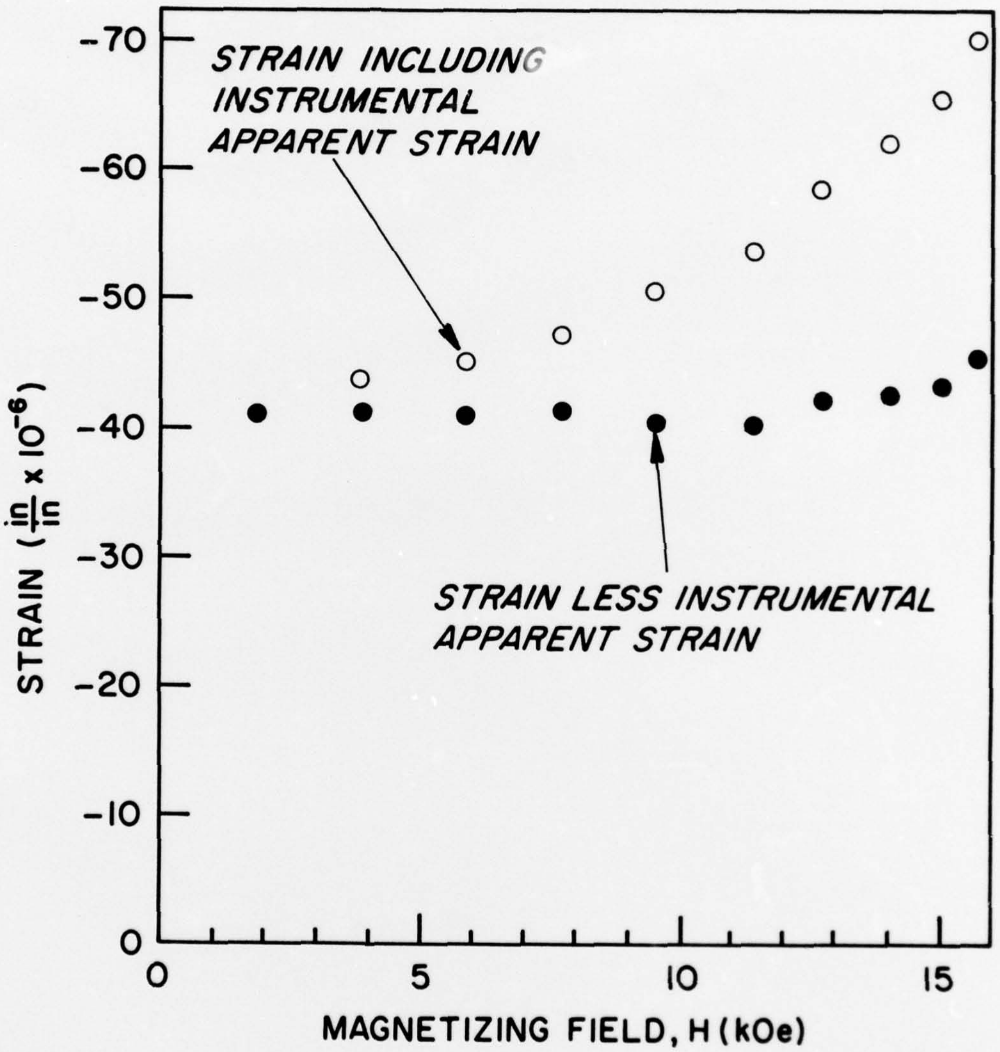

FIGURE 16 - STRAIN AS A FUNCTION OF APPLIED FIELD FOR THE Ni/10% Sm-Fe COMPOSITE EXTRUDED AT 1600°F.

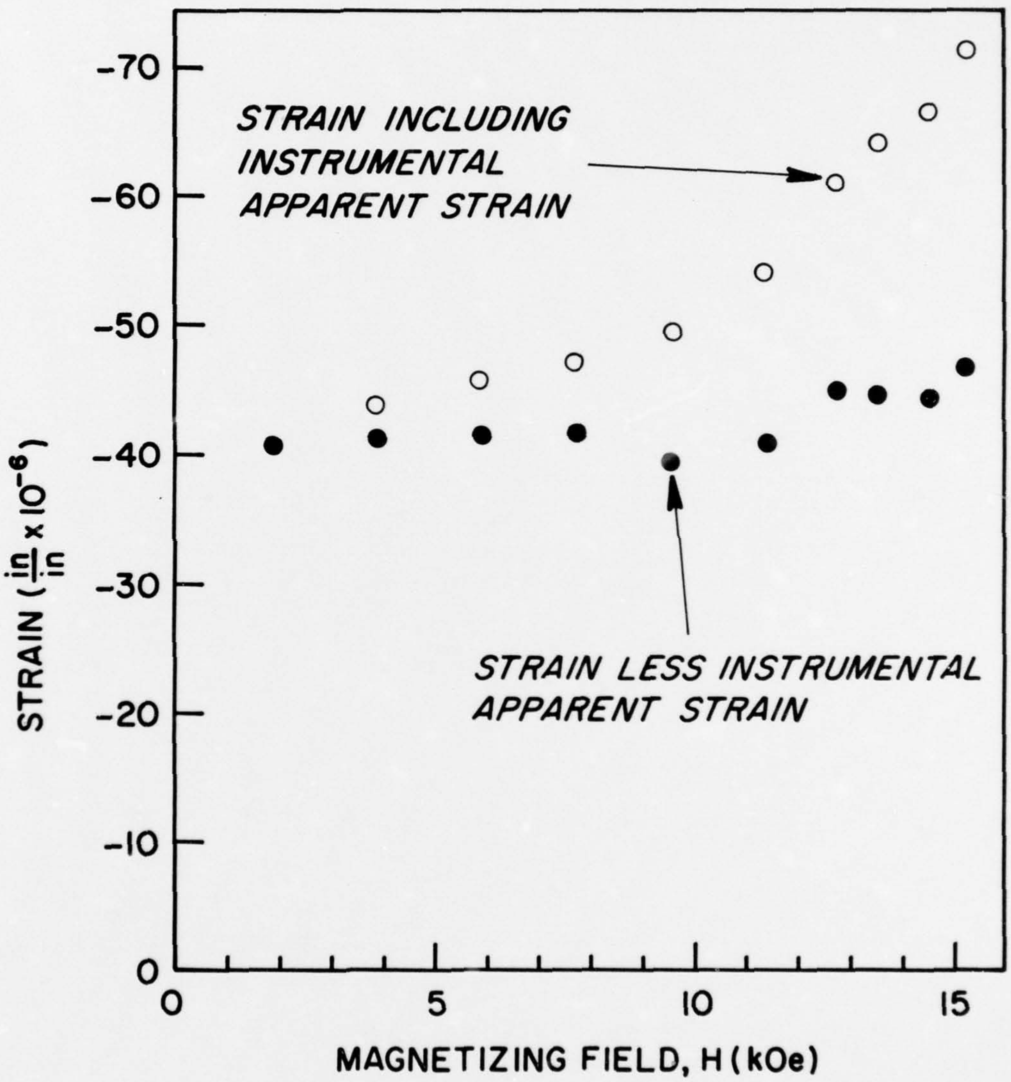

FIGURE 17 - STRAIN AS A FUNCTION OF APPLIED FIELD FOR THE Ni/10% Sm-Fe COMPOSITE EXTRUDED AT 1400°F.

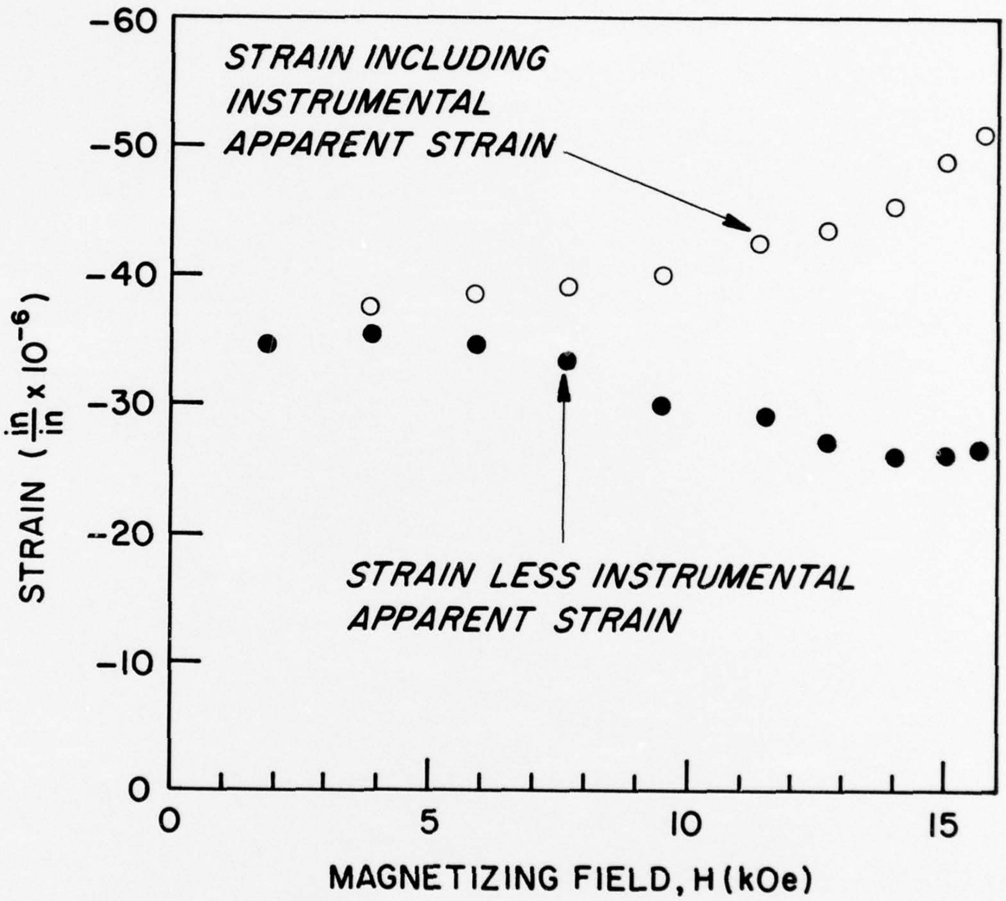

FIGURE 18 - STRAIN AS A FUNCTION OF APPLIED FIELD FOR THE Ni/10% Sm-Fe COMPOSITE EXTRUDED AT 1200°F.

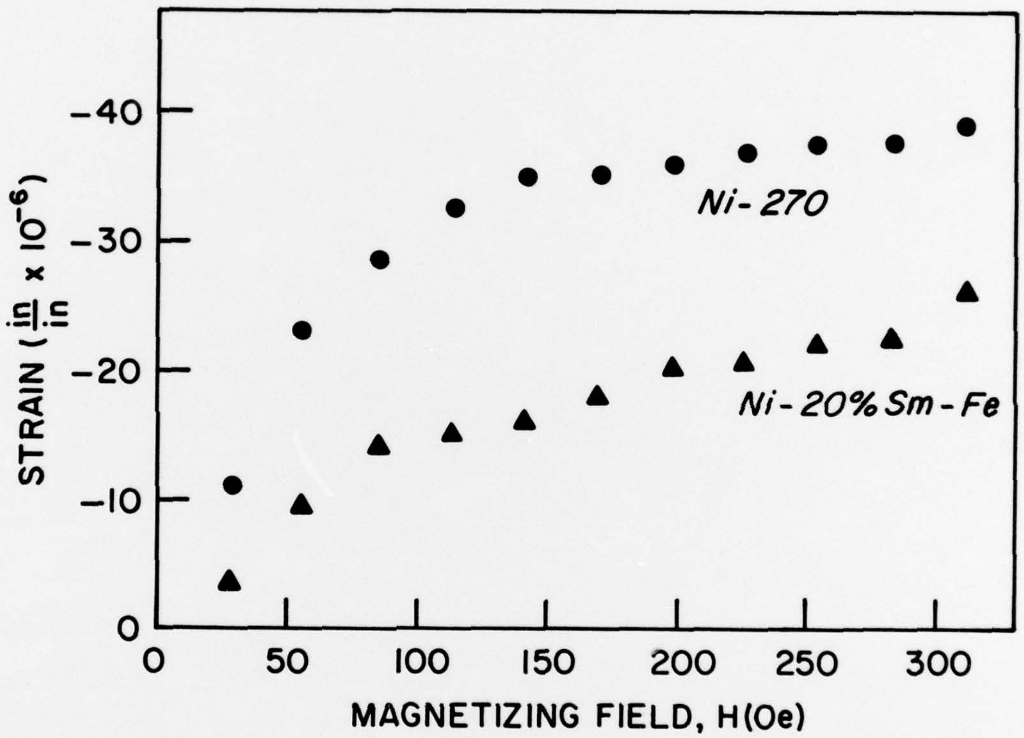

FIGURE 19 - LOW FIELD STRAIN AS A FUNCTION OF APPLIED FIELD FOR THE Ni/20% Sm-Fe COMPOSITE EXTRUDED AT 1400°F.

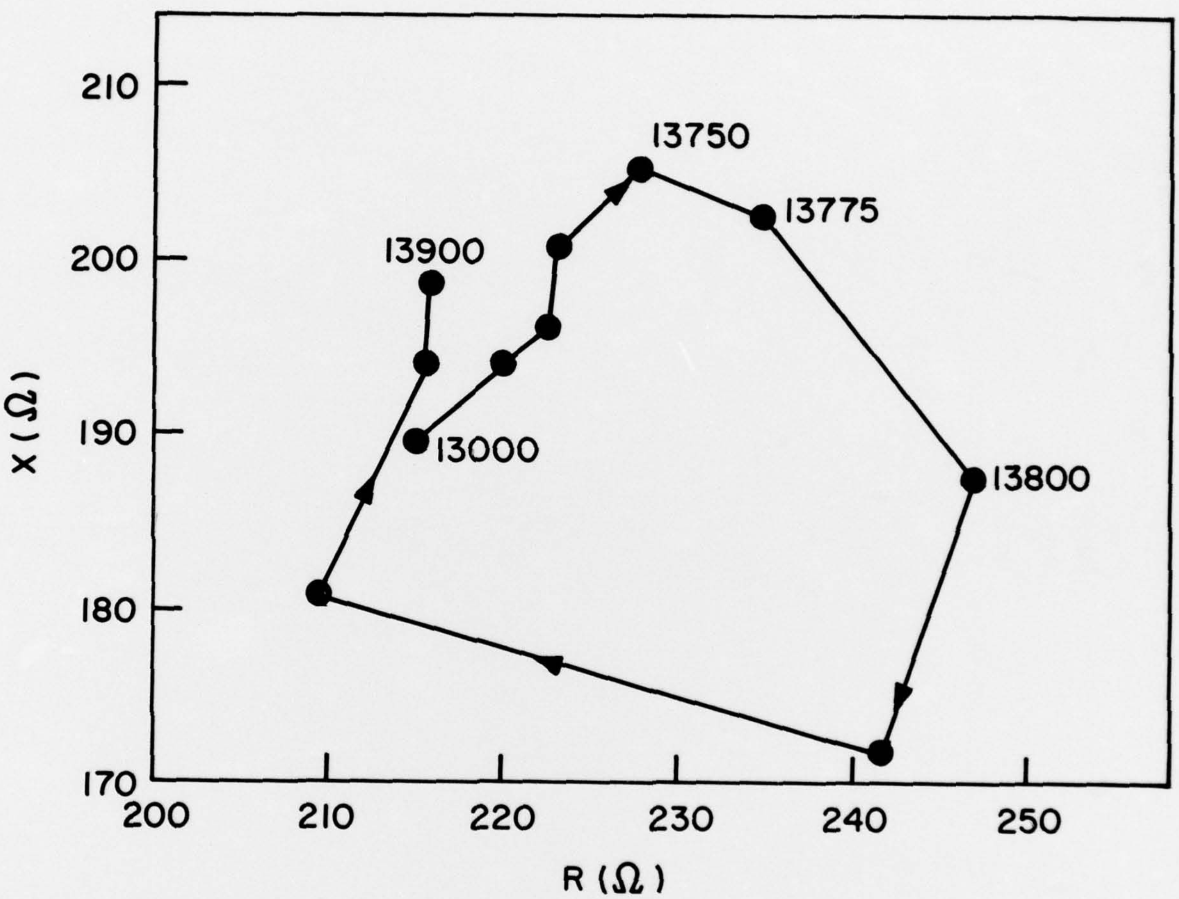

fe ~ 13800

Δf ~ 100

Q = 138

$X_b \approx 200\,\Omega$

0 ~ 35 Ω

$k = \left\{ \frac{35}{200 \times 138} \right\}^{\frac{1}{2}} = \sqrt{.001268}$

$= .0356$

FIGURE 20 - IMPEDANCE MEASUREMENTS FOR THE Ni/20% Sm-Fe COMPOSITE.